Journal of Cleaner Production 228 (2019) 405–417

Contents lists available at ScienceDirect

Journal of Cleaner Production

journal homepage: www.elsevier.com/locate/jclepro

Optimization of a novel liquid-phase plasma discharge process for continuous production of biodiesel

Sarah Wu [a, *], Shaobo Deng [b], Jun Zhu [c], Muhammad Aamir Bashir [a], Forrest Izuno [b]

[a] Biological Engineering, University of Idaho, Moscow, ID, 83844, USA
[b] Southern Research and Outreach Center, University of Minnesota, Waseca, MN, 56093, USA
[c] Biological and Agricultural Engineering, University of Arkansas, Fayetteville, AR, 72701, USA

ARTICLE INFO

Article history:
Received 8 November 2018
Received in revised form
23 April 2019
Accepted 23 April 2019
Available online 26 April 2019

Keywords:
Liquid-phase plasma discharge
Soybean oil
Transesterification
Biodiesel
System optimization

ABSTRACT

The conventional transesterification process employed in biodiesel production from vegetable oils is not only a time-consuming process but operated under raised temperatures. A novel liquid-phase plasma discharge process was developed and evaluated in this study. The process could continuously convert soybean oil to biodiesel under room temperature at a much faster rate than the conventional method. Two feeding flowrates (2.7 ml s^{-1} and 4.1 ml s^{-1}) were used in the experiments. Methanol to oil molar ratio, R_{momr}, and NaOH to oil weight ratio, R_{NaOWR}, were each examined at five levels (3, 4, 5, 6, and 7 for R_{momr}, and 0.4, 0.6, 0.8, 1.0, and 1.2 wt% for R_{NaOWR}). Central Composite Design and Response Surface Methodology to optimize the conversion rate and applied voltage was conducted. At the flowrate of 2.7 ml s^{-1}, the optimal values of R_{momr}, R_{NaOWR}, conversion rate, and applied voltage were 5.08, 0.79 wt%, 97.2%, and 1.17 kV, respectively. While at 4.1 ml s^{-1}, these values became 5.18, 0.70 wt%, 99.74%, and 1.27 kV. All regression models generated by the Central Composite Design and Response Surface Methodology fitted the experimental data well. The biodiesel produced by the novel liquid-phase plasma discharge process met the industrial quality standards (ASTM Standards).

1. Introduction

The importance and significance of reducing the use of petroleum diesel to rein in our reliance on fossil fuels, alleviate the severity of climate change, and protect the environment have long been recognized by both the scientific community and the lay society. The benefits of using biodiesel are well documented including significant reduction in greenhouse gas emissions, non-sulfur emissions and non-particulate matter pollutants, low toxicity, and biodegradable (Mohammed and Bhargavi, 2015). However, with the currently available production technologies, biodiesel cannot secure its fair share with petroleum diesel in the marketplace because of the high cost and low efficiency in the conversion technology (Moazeni et al., 2019). Unless technical breakthroughs take place in the production technology, the current status quo of biodiesel in the transportation fuel market will not change anytime soon.

Among the four available biodiesel production technologies, i.e., direct/blends (Wu et al., 2017), microemulsion (Attaphong et al., 2016), pyrolysis (Laesecke et al., 2017), and transesterification (Musa, 2016; Afzal et al., 2018), transesterification is the most attractive and promising method to chemically convert vegetable oils into biodiesel (Oğuz and Tolu, 2018; De et al., 2019). Transesterification solves the high viscosity problem of the vegetable oil feedstock (Bhuiya et al., 2016; Thoai et al., 2019). Therefore, this technique has been widely accepted by the biodiesel industry with established operations for biodiesel production around the world (Thoai et al., 2019). That said, the transesterification technique itself is not without limitations. It is generally recognized that there are four major factors affecting the biodiesel yield using the transesterification process. These factors include alcohol usage, reaction time, reaction temperature, and catalyst concentration (Nasreen et al., 2018). First, since the transesterification reaction is reversible, an excess amount of alcohol is normally needed to ensure a

Abbreviations: R_{momr}, Methanol to oil molar ratio; R_{NaOWR}, NaOH to oil weight ratio; ASTM, American Society for Testing and Materials; LPPD, Liquid-phase plasma discharge; CCD, Central composite design; RSM, Response surface methodology; ANOVA, Analysis of variance; FAME, Fatty acid methyl ester; API, American Petroleum Institute.

* Corresponding author. Department of Biological Engineering, University of Idaho, 875 Perimeter Drive MS 0904, Moscow, ID, 83844-0904, USA.
E-mail address: xwu@uidaho.edu (S. Wu).

https://doi.org/10.1016/j.jclepro.2019.04.311
0959-6526/

complete conversion of oils to biodiesel. This practice led to an alcohol/oil molar ratio of 6:1 usually adopted (despite that the stochiometric ratio is only 3:1) (Joshi et al., 2019). Second, the reaction temperature needs to be maintained at an elevated level to increase the reaction rate. According to the literature information, regardless of the transesterification methods used (acid or alkali catalytic processes, or non-catalytic supercritical methanol method), the reaction temperature used ranged from around 30 °C–280 °C (usually 50–70 °C for alkali catalysts) (Christian et al., 2018). Third, the reaction time is considered critical to the conversion efficiency of oils to biodiesel. In general, a greater than 98% conversion rate could be achieved in 4 h of reaction time for alkali catalysts (Christian et al., 2018). Finally, catalyst usage could also affect the reaction efficiency because as the catalyst concentration increased, so were the conversion of triglyceride and the yield of biodiesel (Jeyakumar et al., 2018). An optimal catalyst (NaOH) concentration was found to be 1.5 wt% when the maximal yield of biodiesel was reached (Eevera et al., 2009). Considering the operating conditions discussed above in producing biodiesel via transesterification, there is clearly room for improvement to lower the production cost when the biodiesel industry has little control over the cost of raw materials.

To that end, efforts in searching for techniques to improve the transesterification process have debuted in literature in recent years. Azcan and Yilmaz (2012) reported that microwave irradiation could provide intensive heat to the process to effectively accelerate the transesterification reaction rate in production of biodiesel. Ultrasound technology was also studied in biodiesel synthesis because the ultrasonic field was identified to be able to produce chemical and physical effects (Akhtatr et al., 2018). These effects, resulting from the collapse of cavitation bubbles and generating emulsions from immiscible liquids such as oil and alcohol used in biodiesel production, promoted contacts of reactants and improved the reaction rates (Tan et al., 2019). Advantages of using ultrasound processing to produce biodiesel included reduced amounts of alcohol and catalyst required and reduced reaction temperature. The improvement in the transesterification reaction rate (thus reduced production time) in biodiesel synthesis was clearly a promising attribute of this technology (Babajide et al., 2010).

In the meantime, research interest has been growing in studying the use of another technique, i.e., thermal plasma technology, in converting biomass to biofuels (Canabarro et al., 2013). However, the thermal plasma treatment is energy intensive due to the high temperature required to reach the temperature equilibrium among all reactive species involved. To address this issue, researchers use partially discharged corona plasma technique to convert the fatty acids in food wastes to biodiesel (Cubas et al., 2016). Recently, plasma discharge technology was suggested by some researchers in conversion of vegetable oils to biodiesel. They presumed that the electrically-driven ionized gases produced by the electrical discharge should be able to produce chemically active species (Jiang et al., 2014). And these chemical species could act as a bond-breaking catalyst to assist in the propagation of the conversion reactions and lower the temperature required for a reaction to proceed, similar to the reactions observed in the ultrasound technology (Istadi et al., 2014). Given all these good attributes, the research in using the liquid-phase plasma discharge technology in biodiesel production is still blank. A key component central to this endeavor is the lack of innovative liquid-phase plasma discharge reactors that can significantly reduce the processing time in transesterification, while still maintaining good conversion efficiencies and the quality of the biodiesel such produced.

In summary, the current transesterification process is an energy-consuming process with relatively low conversion efficiency in biodiesel production from vegetable oils. In response to the drawbacks of the current technology, the novelty of the proposed liquid-phase plasma discharge process to produce biodiesel from soybean oil includes:

- a new engineering technology in producing biodiesel from vegetable oils that has never been reported
- high conversion efficiency (>99%) with the shortest reaction time (in milliseconds)
- electrical energy use for raising the reaction temperature eliminated
- lower alcohol used
- the quality of biodiesel produced meeting the industrial standards

Therefore, the objectives of this research were to evaluate the performance of the novel liquid-phase plasma discharge (LPPD) process to continuously convert soybean oil to biodiesel that met the industrial standards. Central Composite Design (CCD) coupled with response surface methodology (RSM) was used in the experimental design to examine and optimize two controlling parameters, i.e., the methanol to oil molar ratio (R_{momr}) and the catalyst (NaOH) to oil weight ratio (R_{NaOWR}). Their effects on conversion rates and applied voltages needed to complete the process for biodiesel production were studied. The mechanism of the conversion of soybean oil to biodiesel by LPPD was also briefly discussed.

2. Materials and methods

2.1. Experimental apparatus

Unlike the two most researched configurations of liquid plasma reactors, i.e., pin-to-pin and pin-to-plate (Bruggeman et al., 2016), the liquid-phase plasma discharge (LPPD) reactor used in this study took on a totally different design, which was shown in Fig. 1. This design provided a unique configuration with the high-voltage electrode placed on top of the ground electrode with a dielectric plate separating the two electrodes. A small opening was made in the center of the dielectric plate to concentrate the electrons generated by the electrical discharge in the vicinity of the opening. In so doing, a conducting channel was established and the continuity of the discharge current could be achieved in the form of mobile electrons in the discharge phase (Bruggeman et al., 2007). This design led to better mass transfer and breakdown of substrate

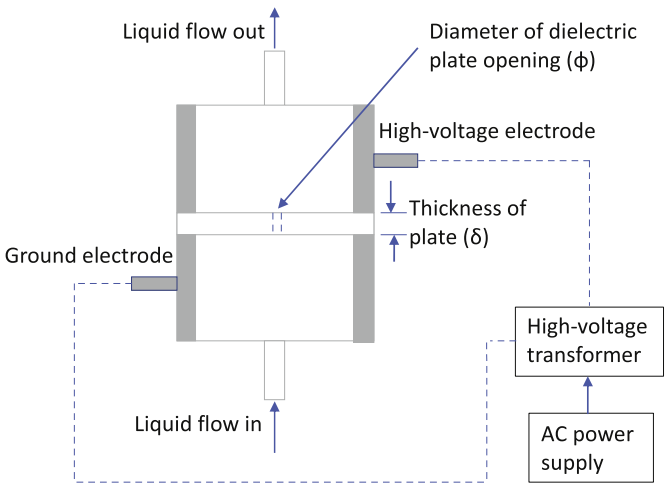

Fig. 1. Schematic of the reactor of LPPD system; $\varphi = 0.8$ mm, $\delta = 3.2$ mm.

molecules in contact with the discharge (Bruggeman et al., 2016). More importantly, this design allowed continuous operation (as compared to batch operation requiring large vessels) with liquid going into the reactor from the bottom and exiting at the top, which could substantially reduce the reactor size and operation costs if scaled up for large productions. The LPPD system consisted of a high-voltage AC transformer (Plasma Technics Inc., Racine, WI 53404, USA), connected to the stainless-steel electrodes on the reactor, to provide high-voltage discharge to the liquid flowing through the reactor, and a peristaltic pump (not shown in Fig. 1) for continuous feeding of the feedstock. The applied power could be adjusted by a transformer regulator. The reactor body was fabricated using polycarbonate material, and the dielectric plate was made of quartz. All experiments were run under room temperature (20–22 °C).

2.2. Experimental design

Two independent variables, i.e., methanol to oil molar ratio (R_{momr}) and NaOH to oil weight ratio (R_{NaOWR}, wt.%), at five levels were examined in this study under two feeding flowrates (2.7 ml s^{-1} and 4.1 ml s^{-1}). Selection of R_{momr} and R_{NaOWR} as the independent variables was to comply with the common parameters used in the conventional transesterification process for biodiesel production (Aransiola et al., 2014). The selection of flowrates was in correspondence to the peristaltic pump speeds of 100 rpm and 150 rpm, respectively. The two pump speeds chosen were based on preliminary trials to ensure that the pump speed fell within the manageable range without losing operability of the LPPD system. Given the two variables (R_{momr} and R_{NaOWR}) with each at five levels, a central composite design (CCD) coupled with response surface methodology (RSM) was employed to determine the optimal controlling values of these two variables to maximize the two response variables, i.e., conversion rate and applied voltage. The five levels of R_{momr} and R_{NaOWR} experimented were 3, 4, 5, 6, and 7, and 0.4 wt%, 0.6 wt%, 0.8 wt%, 1.0 wt%, and 1.2 wt%, respectively. These levels were chosen based on both the literature information and our preliminary experiments. The corresponding coded values were −2, −1, 0, 1, and 2 in the CCD/RSM analysis. The central point values (zero level) chosen for the CCD analysis were $R_{momr} = 5$ and $R_{NaOWR} = 0.8$ wt%.

According to the CCD experimental design, a total of thirteen experiments for each feeding flowrate were conducted for the two independent variables each at five levels with four replicates of the center values. The combinations of controlling variables tested, and the responses obtained were presented in Table 1. A second order quadratic model (Eq. (1)) was used to fit the obtained responses to the experimental variables, which was produced by the regression analysis using the least square method. The Design Expert software (version 11, StatEase, Inc., St. Paul, MN 55413, USA) was employed for all the experimental design and regression analysis.

$$Y = \beta_0 + \beta_1 x_1 + \beta_2 x_2 + \beta_{11} x_1^2 + \beta_{22} x_2^2 + \beta_{12} \times 1 \times 2 \quad (1)$$

Where: Y: the predicted response.

x_1 and x_2: independent variables, R_{momr} and R_{NaOWR}.
β_0: the offset term
β_1 and β_2: linear coefficients
β_{11} and β_{22}: the squared coefficients
β_{12}: the interaction coefficient

For each test, 100 ml of soybean oil added with a proportional volume of methanol was prepared and placed in the influent vessel for the LPPD process. After a short stir-mixing, the mixture was pumping through the reactor. When the power was turned on with a stable plasma discharge, the applied voltage was recorded by an oscilloscope. The effluent from the reactor was collected in a separatory funnel. After a separation time of about 15 min, the bottom liquid portion, consisting of unreacted methanol, glycerol, catalyst, etc., was gravity drained by opening the valve. The top portion of liquid was the methyl esters (biodiesel) produced. The electrical discharge treatment times were determined as 0.5 ms (ms) for flowrate 2.7 ml s^{-1} and 0.3 ms for flowrate 4.1 ml s^{-1}.

2.3. Sampling and analysis

For each experimental run, a biodiesel product sample of 5 ml was taken for fatty acid methyl ester (FAME) analysis to determine the conversion rate as the indicator for the best combination of the test variables. Fatty acids including myristic acid (C14:0), palmitic acid (C16:0), linoleic acid (C18:2), oleic acid (C18:1), stearic acid (C18:0), and arachidic acid (C20:0) went through a FAME derivation process and used as external standards (Indarti et al., 2005). Methyl 2-naphthoate was used as the internal standard (50 μg ml^{-1} in dichloromethane solvent). The prepared FAME derivatives from standard fatty acids and biodiesel samples were analyzed by GC/MS EI (FOCUS-ISQ, ThermoScientific, San Jose, CA95134, USA). The temperature profile for GC was 40 °C (1 min) → 5 °C/min to 320 °C using the GC capillary column of ZB-5MS (30 m, 0.25 mmØ, Phenomenex, Torrance, CA90503, USA). The eluted compounds from biodiesel samples were identified with authentic standards and by

Table 1
Central composite design matrix of the two independent variables in real units with experimental responses for conversion rate (%) and applied voltage (kV) for the two flowrates.

Run	Flowrate: 2.7 ml s^{-1}				Flowrate: 4.1 ml s^{-1}			
	R_{momr}	R_{NaOWR} (wt.%)	Conv. rate (%)	Applied voltage (kV)	R_{momr}	R_{NaOWR} (wt.%)	Conv. rate (%)	Applied voltage (kV)
1	5.0	0.80	96.56	1.08	5.0	0.80	98.76	1.23
2	7.0	1.20	82.13	1.69	3.0	1.20	82.41	2.36
3	5.0	1.37	79.23	2.12	5.0	0.80	94.68	1.37
4	5.0	0.80	98.67	1.13	5.0	0.23	89.58	1.97
5	7.0	0.40	87.90	1.67	5.0	1.37	75.45	2.01
6	3.0	0.40	79.78	1.78	7.8	0.80	79.73	2.12
7	2.2	0.80	90.23	1.97	5.0	0.80	99.81	1.15
8	5.0	0.80	98.77	1.14	5.0	0.80	99.73	1.45
9	5.0	0.80	95.13	1.17	2.2	0.80	75.11	1.78
10	5.0	0.23	83.13	2.24	7.0	1.20	75.36	2.14
11	7.8	0.80	95.78	2.03	7.0	0.40	90.23	1.69
12	5.0	0.80	96.45	1.43	5.0	0.80	99.69	1.49
13	3.0	1.20	85.60	2.37	3.0	0.40	85.66	1.89

spectral matching with the 2008 NIST mass spectral library (Osman et al., 2012). The conversion rate was calculated using the following equation:

$$C = \frac{(\sum A) - A_{EI}}{A_{EI}} \times \frac{C_{EI} \times V_{EI}}{W} \times 100\% \quad (2)$$

where $\sum A$ —total peak area of methyl ester, A_{EI}— peak area of methyl 2-naphthoate, C_{EI}—concentration (mg/mL) of internal standard solution, V_{EI}—volume (mL) internal standard solution and W—weight (mg) of sample.

Analysis of one biodiesel sample for comparison with the ASTM Standards was performed by a commercial service company, the MEG Corp Consulting (Plymouth, MN 55441, USA). The methods used to test the biodiesel sample by the consulting firm were presented in the ASTM Standards (D6571) and the European Standards (EN 14112) for different factors such as D288 for American Petroleum Institute (API) gravity, D2500 for cloud point, D2709 for water, EN15751 for oxidation stability, D664 for total acid number, and D6584 for free and total glycerin (EN, 2016; ASTM, 2018). The results were compared to the specifications set forth in the ASTM Standards (D6751) for biodiesel quality.

3. Results and discussion

3.1. Quadratic model development based on the CCD and RSM data

The central composite design (CCD) in the Design-Expert software generated four quadratic models for the two independent variables (R_{momr} and R_{NaOWR}) tested in this study under two different liquid flowrates. The results showed that these models were able to fit the two response variables (conversion rate and applied voltage) relatively well. Apart from the model fitting results, the ANOVA analysis performed on the fitted quadratic equations also revealed the significant relationships between the independent and response variables as shown below.

First, the quadratic expressions of the models for the conversion rate and applied voltage with R_{momr} and R_{NaOWR} as independent variables were presented in Eq. (3) through Eq. (6) for the two different liquid flowrates used in the experiment. All the coefficients (β_is) in these equations were determined by the regression analysis of the experimental data performed by the Design-Expert software.

For the flowrate of 2.7 ml s^{-1}, the regression equations using actual factors (ditto) for the two response parameters were:

$$R_{conv} = 27.29 + 10.80R_{momr} + 103.96R_{NaOWR} - 3.59R_{momr}{}^{*}R_{NaOWR} - 0.71R_{momr}^2 - 54.83R_{NaOWR}^2 \quad (3)$$

$$V_{Applied\ voltage} = 4.55 - 0.78R_{momr} - 3.39R_{NaOWR} - 0.18R_{momr}{}^{*}R_{NaOWR} + 0.09R_{momr}^2 + 2.76R_{NaOWR}^2 \quad (4)$$

For the flowrate of 4.1 ml s^{-1}, the regression equations for the two response parameters were:

$$R_{conv} = 3.08 + 27.40R_{momr} + 77.73R_{NaOWR} - 3.63R_{momr}{}^{*}R_{NaOWR} - 2.42R_{momr}^2 - 44.67R_{NaOWR}^2 \quad (5)$$

$$V_{Applied\ voltage} = 4.39 - 0.78R_{momr} - 3.05R_{NaOWR} - 0.006R_{momr}{}^{*}R_{NaOWR} + 0.08R_{momr}^2 + 2.11\ R_{NaOWR}^2 \quad (6)$$

Where: R_{conv} is oil conversion rate (%); R_{momr} and R_{NaOWR} were defined early; $V_{Applied\ voltage}$ is applied voltage (kV).

Second, according to the results of ANOVA analyses for Eq. (3) through 6 presented in Table 2, all models demonstrated a significant goodness-of-fit with F values ranging from 7.16 to 29.12. The corresponding P values ranged from 0.0002 to 0.0112 (<0.05). In general, the goodness-of-fit of regression models for conversion rate for both flowrates was better than those for applied voltage because the F values for the former were much larger than those for the latter (24.05 and 29.12 vs. 8.85 and 7.16). Another important factor with respect to determining the goodness-of-fit for regression models was to examine the "lack of fit" analysis results. As shown in Table 2, all P values for the lack of fit tests were greater than 0.05 (ranging from 0.0877 to 0.2112), which was considered insignificant. Also, additional experiments were conducted to verify the models by correlating the modeled with the observed responses (Fig. 2). The coefficients of determination for the four responses ranged from 0.8472 to 0.9516. This indicated that even the regression model with the lowest coefficient of determination (in this case, the applied voltage response for the flowrate of 2.7 ml s^{-1}) could still explain 84.72% of the response variability if the model was used to simulate the experiment. The other three surface response models can explain 93.09%, 95.16%, and 92.17% of the variability for the conversion rate for flowrates of 2.7 ml s^{-1} and 4.1 ml s^{-1}, and the applied voltage for the flowrate of 4.1 ml s^{-1}, respectively. As such, it can be concluded that all these quadratic regression models generated by the CCD/RSM analysis are able to fit the experimental data relatively well. These models can be used to adequately describe the effects of the two independent parameters (R_{momr} and R_{NaOWR}) on the soybean oil conversion process with respect to conversion rate and applied voltage to produce biodiesel using the LPPD process evaluated in this study.

To further examine the goodness-of-fit of the regression models, more parameters in addition to R^2, F, and P values were also examined. These parameters included adjusted R^2, adequate precision, and coefficient of variation (C.V.) (Table 2). The adjusted R^2 for the regression models for the two flowrates (2.7 mg s^{-1} and 4.1 mg s^{-1}) were 0.9057 and 0.9214 (conv. rate) and 0.7659 and 0.7197 (applied voltage), respectively. For the conversion rate, over 90% of variation in the prediction could be explained by the variation in independent variables, while for the applied voltage, such percentages of explanation were reduced to 76.59 and 71.90% for the two flowrates. This information showed that for conversion rate in both cases, the goodness-of-fit of the models was robust, while that for the applied voltage was slightly lower. In the same way, the coefficients of variation for these models also showed that the two models for the conversion rates were much better than the other two for the applied voltage (2.51% and 3.14% vs. 13.1% and 11.55%) in precisely determining the response variables based on the independent variables in simulation (Lehmann and Romano, 2008). In addition to these observations, the adequate precision values for all models were greater than 4.0 (indicating adequate signals). This inferred that these models could sufficiently predict the values of responses within the design space defined in the experimental design in this study (Draper and Smith, 1998). That said, it is expected that the two applied voltage models may present a wider spread of data around the means in making predictions.

The ANOVA analysis of the effects of the two variables in the regression equations from (3) to (6) as well as their interactions was presented in Table 3. The results showed that for flowrate 2.7 ml s^{-1}, the P values were ranging from <0.0001 to 0.0432, all of which were smaller than 0.05. This indicated that the two variables, their interactions, and their quadratic forms all had a significant impact on the response variables (conversion rate and applied voltage). The interacting effect of R_{momr} and R_{NaOWR} could be verified by the contours shown in Fig. 3a and b, where they showed an elliptical shape. For flowrate 4.1 ml s^{-1}, all P values were also smaller than 0.05 except one, which was the interacting effect between R_{momr} and R_{NaOWR} for the applied voltage. This indicated

Table 2
ANOVA analysis for fitting models for conversion rate and applied voltage under the two flowrates tested.

Model ANOVA Analysis	Response Variables			
	Conv. rate[§] (2.7 ml s^{-1})	Applied voltage (2.7 ml s^{-1})	Conv. rate[§] (4.1 ml s^{-1})	Applied voltage (4.1 ml s^{-1})
Sum of squares	612.33	2.14	1116.10	1.45
Mean squares	122.47	0.43	223.22	0.29
R square	0.9450	0.8635	0.9541	0.8365
Adjusted *R* square	0.9057	0.7659	0.9214	0.7197
Mean	89.96	1.68	88.17	1.74
Std. deviation	2.26	0.2198	2.77	0.2012
C.V. (%)	2.51	13.1	3.14	11.55
Adeq Precision	12.094	7.229	12.763	6.217
SSE*	35.68	0.2921	51.23	0.2371
F value	24.05	8.85	29.12	7.16
P value	0.0003	0.0062	0.0002	0.0112
Lack of fit				
F value	3.490	4.580	2.370	3.180
P value	0.1291	0.0877	0.2112	0.1465

* Sum of squared errors of prediction.
§ Conversion rate was calculated using Eq. (2).

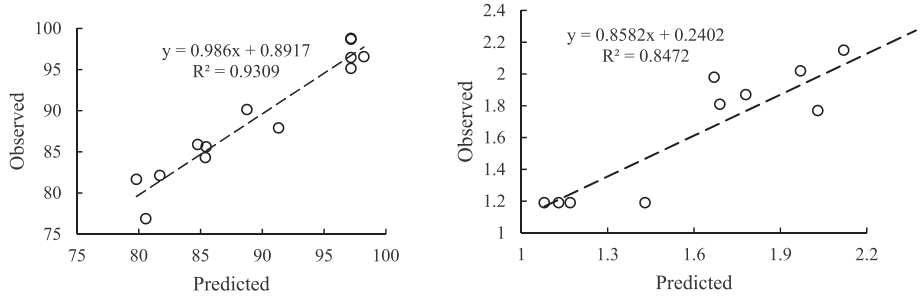

(a)

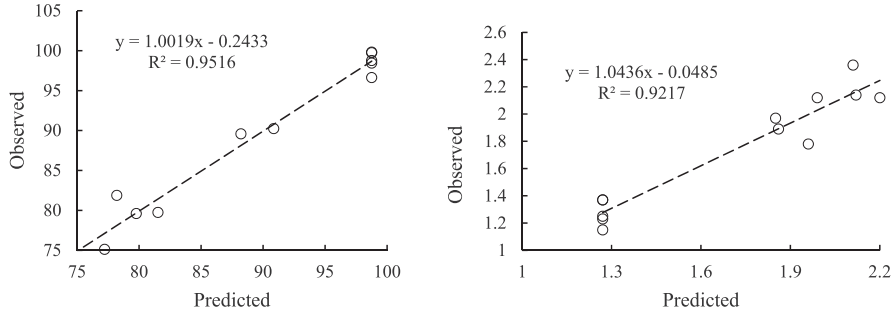

(b)

Fig. 2. The linear correlations between the observed and predicted data for flowrate 2.7 ml s^{-1} (a), and 4.1 ml s^{-1} (b), with conversion rate on the left and applied voltage on the right.

that the effect of interaction between the two variables was insignificant for the applied voltage response, as seen in Fig. 3d, in which the shapes of contours were largely circles.

Finally, the residuals of model fitting regressions using ANOVA were illustrated in Fig. 3. The random pattern of the residual distribution for all graphs was clearly typical of the pattern for good regression results (Mendenhall and Sincich, 2012). The residual data points were largely symmetrically distributed, tending to cluster towards the middle of the plots but without clear patterns in general. Therefore, the data presented in Fig. 3 supported the observations obtained early that the regression models developed could adequately predict the responses within the experimental conditions defined in this study.

3.2. Responses of conversion rate and applied voltage to the test variables

Fig. 4 presented the surface response plots of conversion rate and applied voltage with respect to the two independent variables (R_{momr} and R_{NaOWR}). Clearly, the ranges for these two variables

Table 3
ANOVA analysis for model variables and their interactions for conversion rate and applied voltage under the two flowrates tested.

Model ANOVA Analysis (Conversion rate)	Response Variables (2.7 ml s^{-1})				
	A (R_{momr})	B (R_{NaOWR})	A x B	A^2	B^2
Sum of squares	29.25	33.86	33.06	56.90	535.34
Mean squares	29.25	33.86	33.06	56.90	535.34
F – value	5.74	6.65	6.49	11.17	105.11
P – value	0.0413[a]	0.0313[a]	0.0382[a]	0.0124[a]	<0.0001[a]
(Applied voltage)					
Sum of squares	0.622	0.242	0.812	0.861	1.36
Mean squares	0.622	0.242	0.812	0.861	1.36
F – value	12.87	5.01	16.80	17.83	28.12
P – value	0.0095[a]	0.0432[a]	0.0041[a]	0.0039[a]	0.0011[a]
Model ANOVA Analysis (Conversion rate)	Response Variables (4.1 ml s^{-1})				
	A (R_{momr})	B (R_{NaOWR})	A x B	A^2	B^2
Sum of squares	42.05	181.48	43.76	653.88	355.40
Mean squares	42.05	181.48	43.76	653.88	355.40
F – value	5.48	23.67	5.71	85.30	46.36
P – value	0.0426[a]	0.0018[a]	0.0417[a]	<0.0001[a]	0.0003[a]
(Applied voltage)					
Sum of squares	0.512	0.3122	0.0001	0.7057	0.7971
Mean squares	0.512	0.3122	0.0001	0.7057	0.7971
F – value	12.65	7.71	0.0025	17.44	19.69
P – value	0.0113[a]	0.0287[a]	0.9617	0.0042[a]	0.0030[a]

[a] means that the coefficients are significant.

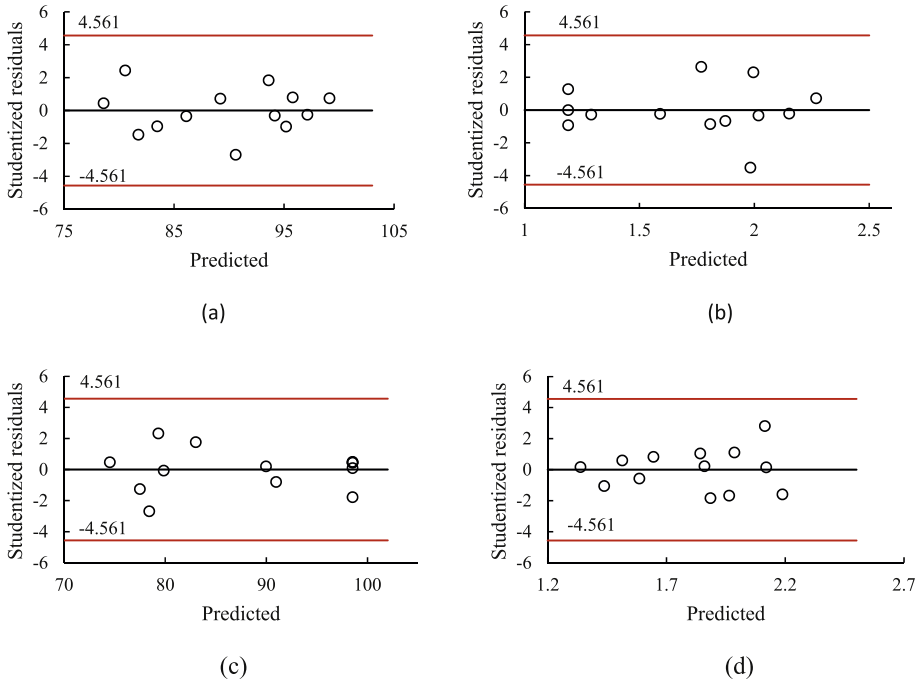

Fig. 3. The predicted vs. studentized residuals; (a) and (b), conversion rate and applied voltage for flowrate 2.7 ml s^{-1}; (c) and (d), conversion rate and applied voltage for flowrate 4.1 ml s^{-1}.

selected for examination in this study were appropriate because the optimal values of the response variables (conversion rate and applied voltage) were captured adequately from the experimental design. For the flowrate of 2.7 ml s^{-1}, the optimal values of R_{momr} and R_{NaOWR} were 5.64 and 0.77 wt%, respectively, which produced the optimal conversion rate of 97.55% (Table 4). While for the flowrate of 4.1 ml s^{-1}, the optimal R_{momr} and R_{NaOWR} values were 5.16 and 0.67 wt% to achieve the optimal conversion rate of 99.51%. In both cases, the corresponding applied voltage responses were 1.26 kV and 1.38 kV, respectively. Please note that these R_{momr} and R_{NaOWR} values were not the optimal values for the applied voltage variable. Instead, the optimal values of R_{momr} and R_{NaOWR} for applied voltage were 5.25 and 0.79 wt% for flowrate 2.7 ml s^{-1}, and 4.99 and 0.73 wt% for flowrate 4.1 ml s^{-1} (Table 4). Carefully examining the contour plot in Fig. 4a revealed that the area enclosed by the smallest circle represented a conversion rate of at least 97.32%, which was virtually very close to the optimal value (97.55%) determined at the center of the circle. It can thus be inferred that if achieving a conversion rate of equal to or greater than 97.32% is satisfactory, the combined values of R_{momr} and R_{NaOWR} can be chosen anywhere inside the smallest contour circle shown in Fig. 4a. Therefore, instead of arriving at a single combination, a range of

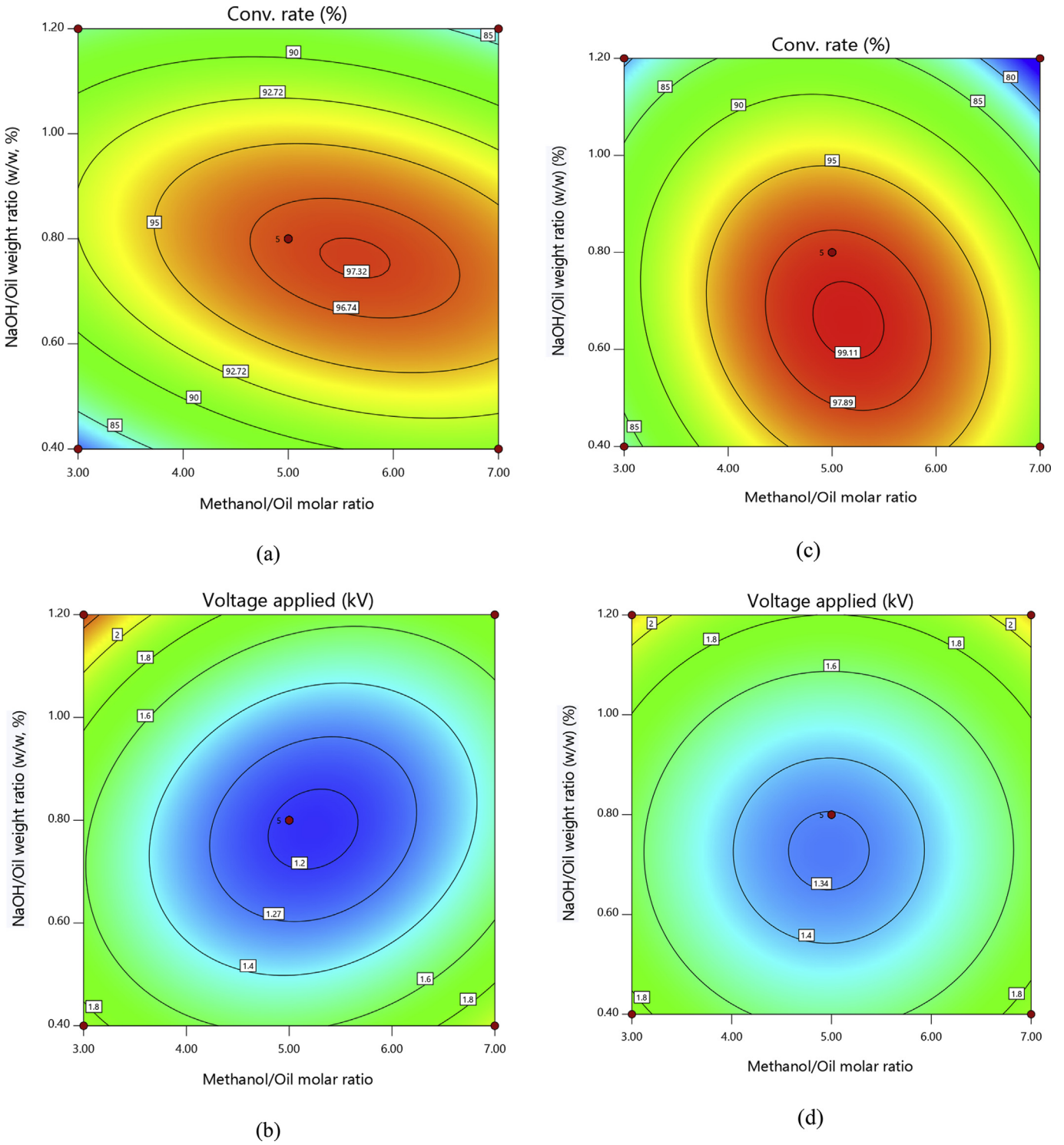

Fig. 4. The response surface plots of conversion rate and applied voltage with respect to R_{momr} and R_{NaOWR} for flowrate 2.7 ml s^{-1} (a and b) and 4.1 ml s^{-1} (c and d).

R_{momr} and R_{NaOWR} values that can be used to achieve the optimal conversion rate (≥97.32%) can be established, which is 5.30–5.97 for R_{momr} and 0.73–0.80 wt% for R_{NaOWR}, respectively. Similarly, the optimal range of values for R_{momr} and R_{NaOWR} to guarantee an applied voltage that is equal to or smaller than 1.20 kV is 4.80–5.67 for R_{momr} and 0.71–0.86 wt% for R_{NaOWR}, respectively. For the flowrate of 4.1 ml s^{-1}, the optimal ranges for R_{momr} and R_{NaOWR} values were 4.81–5.50 and 0.58–0.74 wt% to achieve a conversion rate equal to or greater than 99.11%, and 4.56–5.39 and 0.65–0.81 wt% to achieve an applied voltage equal to or smaller than 1.35 kV (Fig. 4 and Table 4).

There are reports in literature about optimizing the transesterification process of producing biodiesel from soybean oil using the CCD/RSM methodology. One study by Silva et al. (2011) reported that the best conversion rate of soybean oil to biodiesel obtained using conventional transesterification was 95% under the

Table 4
Optimum conditions and responses for tested parameters.

Optimized responses	R_{momr}	R_{NaOWR} (wt.%)	Conv. ratio (%, 2.7 ml s^{-1})	Appl. voltage (kV, 2.7 ml s^{-1})	Conv. ratio (%, 4.1 ml s^{-1})	Appl. voltage (kV, 4.1 ml s^{-1})
Conv. ratio (%, 2.7 ml s^{-1})	5.64 (5.30 −5.97)	0.77 (0.73 −0.80)	97.55 (≥97.32)	1.26	–	–
Applied voltage (kV, 2.7 ml s^{-1})	5.25 (4.80 −5.67)	0.79 (0.71 −0.86)	97.24	1.18 (≤1.20)	–	–
Conv. ratio (%, 4.1 ml s^{-1})	5.16 (4.81 −5.50)	0.67 (0.58 −0.74)	–	–	99.51 (≥99.11)	1.38
Applied voltage (kV, 4.1 ml s^{-1})	4.99 (4.56 −5.39)	0.73 (0.65 −0.81)	–	–	99.26	1.33 (≤1.35)

conditions of R_{momr} 9:1, R_{NaOWR} 1.3 wt%, temperature 40 °C, and reaction time 80 min. Compared to the optimal values for the same parameters in this study, i.e., 4.99–5.64 for R_{momr}, 0.67–0.79 wt% for R_{NaOWR}, 20–22 °C for temperature, and 0.5 ms for reaction time, their system would require much more methanol, catalyst, and electricity to raise temperature to operate to only achieve 95% conversion rate as opposed to the >97% conversion rates achieved by the LPPD system reported herein. Several other studies even showed much higher values of R_{momr} (6:1–12:1), R_{NaOWR} (1.3–1.5 wt%), temperature (40–75 °C), and reaction time (40 min–2 h), with the conversion rate ranging from 67 to 98% (Noureddini and Zhu, 1997; Antolın et al., 2002; Yin et al., 2008). With reference to all these results, the LPPD system developed and evaluated in this study was certainly advantegeous and promising.

Techniques to improve the transesterification efficiency were also evaluated by previous workers. As stated early, the ultrasound technology could produce chemical and physical effects originating from the collapse of cavitation bubbles. This activity helped increase mixing between the reactants, thus improving the reaction rates (Istadi et al., 2014). For this reason, Santos et al. (2009) did an optimization study where ultrasound was employed to assist in the transesterification of soybean oil to biodiesel. They reported a nearly 100% conversion rate achieved under the optimal conditions of R_{momr} 9:1, R_{NaOWR} 0.2 wt%, temperature 29 °C, and reaction time 30 min. Apparently, these results were better than those reported by Silva et al. (2011) above, but all values of the running parameters, except R_{NaOWR}, were higher than the ones used in this study. Besides ultrasound, microwave technology was also evaluated by researchers to help improve the transesterification process in biodiesel production from soybean oil. Li et al. (2013) documented a study using a zirconia catalyst in a microwave chemical reactor to promote the transesterification reaction. The optimal biodiesel yield achieved was 94% under the conditions of R_{momr} 2:1, R_{NaOWR} 10 wt%, temperature 65 °C, and reaction time 30 min. Although R_{momr} was reduced to 2:1, the excessive amount of catalyst added and the high temperature required to obtain the optimal yield were discouraging. The reaction time of 30 min as a result of microwave treatment was a great improvement as compared to that in conventional transesterification. But it was only on par with that used in the ultrasound assisted transesterification process, and was much longer than the reaction time needed for the LPPD process experimented in this study. After reviewing all these past techniques attempted by the previous researchers, it can be concluded that the LPPD system developed and evaluated in this study is the most promising technique among the available techniques in promoting the transesterification process to convert soybean oil to biodiesel. Further research to develop it into an applicable technology at the commercial scale is thus warranted.

Comparing the data in Table 4 for the two liquid flowrates studied also revealed another scenario, i.e., a higher conversion rate could be achieved if a higher flowrate was used (97.55% and 99.51% for flowrates of 2.7 ml s^{-1} and 4.1 ml s^{-1}). However, a higher applied voltage was also needed associated with the higher flowrate used (1.33 kV vs. 1.18 kV). This indicated that an improvement of conversion rate by 2.04% would give rise to an increase of applied voltage by 12.7% (six-folds). This meant that the energy efficiency could be reduced as the liquid flowrate increased. Although the LPPD technology has not been used in biodiesel production from soybean oil according to the current literature, the research on using this technology to treat industrial wastewater has been reported in the scientific communities in recent years. Reviewing the available literature showed that the energy efficiency for the LPPD technology was somewhat dependent on the design of the reactor. Patinglag et al. (2018) studied a dielectric barrier discharge reactor to treat methylene blue in water and found that the energy efficiency decreased with increasing water flowrate. While others reported an increase in energy efficiency with an increasing water flowrate when an AC gliding arc discharge reactor was used to treat wastewater containing 4-chlorobenzoic acid (Lesage et al., 2013). Another study even suggested the existence of an optimal water flowrate based on the data evaluating the effect of flowrate on wastewater treatment using a pulsed discharge type reactor (Sugai et al., 2015). Referring to these reports, the results from this study were considered consistent with the results from the previous studies. That said, since energy efficiency is a response variable in the LPPD reactor design, it is possible to improve the current reactor design in this study to enhance energy efficiency without sacrificing the conversion rate. However, a higher flowrate means a higher throughput capacity of the conversion system. This may offset some of the loss in energy efficiency from the angle of economics for practical applications. More facts-finding research is clearly called for in this area.

An interesting observation could be obtained from the optimization data shown in Table 4. Namely, there was no single combination of R_{momr} and R_{NaOWR} values present for simultaneously optimizing both response variables. For instance, the optimal R_{momr} and R_{NaOWR} values for achieving the optimal conversion rate for flowrate 2.7 ml s^{-1} were not the same as those for achieving the optimal applied voltage. Similar statements could also be made for the data obtained under flowrate 4.1 ml s^{-1}. It must be understood that one LPPD process can only be operated using one set of the controlling parameters. Many optimization studies of either a system or a device are normally focused on a single response variable, rather than optimizing two or more response variables using the same controlling parameter(s) at the same time. In the case of flowrate 2.7 ml s^{-1} in this study, if the controlling values of R_{momr} and R_{NaOWR} were set at 5.64 and 0.77 wt% to achieve the optimal conversion rate, the applied voltage would deviate from its optimal value of 1.18–1.26 kV, an increase by 6.78%. On the contrary, if the controlling values of R_{momr} and R_{NaOWR} were selected to be 5.25 and 0.79 wt% to achieve the optimal applied voltage, the deviation of the conversion rate from its optimal value would be 0.32% (from

97.55% to 97.24%). Now the question comes down to whether a reconciled optimal condition can be selected, which can reduce the deviations of both response variables from their respective optimal values to the minimum. With this criterion in mind, the best possible combination of R_{momr} and R_{NaOWR} can be determined based on the information presented in Table 4 and Fig. 4 from this study. Since there was an overlap in R_{momr} and R_{NaOWR} between the two response variables, a reconciled operating condition could be found in the overlapped region to ensure the best possible performance of the liquid electrical discharge process for both response variables. A simple calculation based on the data generated by the Design-Expert software resulted in a different selection of the values for R_{momr} and R_{NaOWR}, i.e., 5.49 and 0.78 wt%. And the optimal conversion rate and applied voltage were 97.42% and 1.26 kV (only 0.1% off of the optimal responses of 97.55% for the former and 6.78% for the latter). Clearly, the optimal conversion rate and applied voltage achieved under this running condition were able to accommodate the differences found under the conditions for optimizing either the conversion rate alone or the applied voltage alone, as shown above. In the same way, the reconciled values of R_{momr} and R_{NaOWR} for the liquid flowrate of 4.1 ml s^{-1} were 5.23 and 0.69 wt%, respectively. This led to a conversion rate of 99.45% (only 0.06% lower than the optimal value) and an applied voltage of 1.37 kV (only 2.71% higher than the optimal value). Therefore, the information generated from this study can provide useful knowledge for further studies in optimizing multiple response variables to achieve optimization for the targeted system.

To confirm the above reconciled optimal conditions for the two flowrates, i.e., 2.7 ml s^{-1} and 4.1 ml s^{-1}, additional experiments were run using the reconciled control parameters ($R_{momr} = 5.49$, $R_{NaOWR} = 0.78$ wt% for 2.7 ml s^{-1} and $R_{momr} = 5.23$, $R_{NaOWR} = 0.69$ wt% for 4.1 ml s^{-1}). For each flowrate examined, the experiment was conducted in triplicate. The results showed that for 2.7 ml s^{-1}, the average conversion rate was 97.53 ± 1.33%, and the average applied voltage was 1.23 ± 0.03 kV. For 4.1 ml s^{-1}, the average conversion rate was 99.63 ± 0.10% and the average applied voltage obtained was 1.36 ± 0.01 kV. These results confirmed that the optimal reconciled operating conditions in terms of R_{momr} and R_{NaOWR} for the novel liquid-phase plasma discharge process were valid, and the conversion rates and the applied voltages obtained using these controlling values were all within the optimal range described previously.

Lastly, it might be interesting to further examine the relationship between the conversion rate and the applied voltage for the LPPD system evaluated in this study to produce biodiesel from soybean oil (Fig. 5). It appeared that when the applied voltage was below around 1.38 kV, the conversion rate stayed consistently higher than 95% for both flowrates (2.7 ml s^{-1} and 4.1 ml s^{-1}). When the applied voltage went above 1.38 kV, a drastic drop in conversion rate was observed. And the decreasing trend continued until the applied voltage increased to around 2 kV. After that, the conversion rate began to increase gradually with the increase in the applied voltage (as shown by the dotted line in Fig. 5). A few comments may be made on this observation. First, it appeared that in order to obtain a high conversion rate for the LPPD process examined in this study, the applied voltage should not exceed 1.38 kV. Since increasing applied voltage would increase the electrical current through the LPPD reactor (assuming that the system resistance remained constant), keeping a low applied voltage was thus advantageous to save energy. Second, when the applied voltage was kept below 1.38 kV, it seemed that the conversion rate was not affected by the liquid flowrate. This suggested that the LPPD process might be able to handle a flowrate higher than 4.1 ml s^{-1}, while still maintaining its conversion rate above 95%. Increasing the flowrate of the LPPD system without increasing energy input is clearly beneficial because it can increase the throughput capacity and the overall efficiency of the system. However, since only two flowrates were studied herein, the level of increase in flowrate beyond 4.1 ml s^{-1} without compromising the conversion rate could not be determined. Finally, although the conversion rate went back up after the applied voltage passed 2 kV, it did not seem to be able to regain the 95% conversion rate based on the data shown in Fig. 5. These observations certainly warrant further research on the LPPD process.

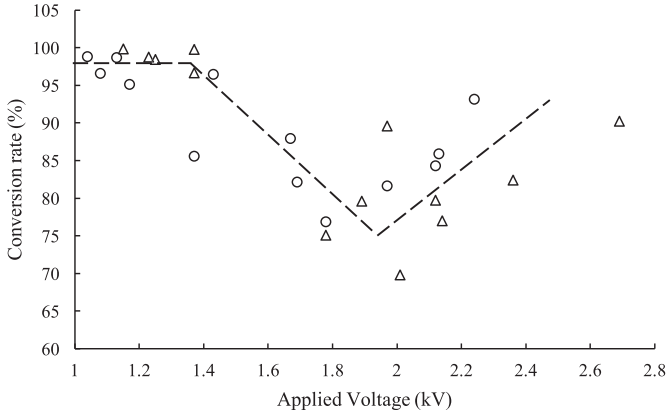

Fig. 5. The relationship between the conversion rate and applied voltage for the LPPD process studied; ○ - flowrate 2.7 ml s^{-1}; Δ - flowrate 4.1 ml s^{-1}.

3.3. Inference of the mechanism behind biodiesel production by the LPPD process and the biodiesel quality compared to that produced by conventional transesterification

Today, biodiesel around the world is mostly produced by a well-known process called "transesterification" (Di Serio et al., 2007). This process, catalyzed by methanol and an alkaline catalyst such as NaOH, converts the triglycerides in refined/edible oils to a mixture of fatty acid methyl esters (FAME), which is called biodiesel (Thanh et al., 2012). The commonly identified bottlenecks in using the conventional transesterification technology to manufacture biodiesel is the high reaction temperature (>60 °C) and long reaction time (2–10 h) (Borges and Díaz, 2012; Moazeni et al., 2019). Since the LPPD reactor used to synthesize biodiesel in this study only ran for less than a second (rather than hours) under room temperature (~20 °C instead of 60 °C), a legitimate question to ask here is whether this process followed the transesterification mechanism to produce biodiesel. This question might be answered by examining and comparing the final biodiesel products from the two production methods, i.e., conventional vs. LPPD.

Fig. 6 presented the analysis data by gas chromatography of the biodiesel products produced using both the conventional transesterification technology and the LPPD process evaluated in this study. Comparing Fig. 6a and b indicated that these two graphs virtually overlapped each other entirely, with the numerical values of all peaks being very similar. This observation could imply that the reactions taking place in the LPPD to synthesize biodiesel could also be a transesterification process because both biodiesel samples demonstrated exactly the same chemical composition. According to literature, transesterification is a three-step process, i.e., triglycerides ⇔ diglycerides ⇔ monoglycerides ⇔ glycerol + FAME. It takes time to reach equilibriums for each of these reactions, and the dynamic changes in the quantity of each reactant and/or product could affect the individual reaction speed, which determines the overall transesterification reaction rate (Arumugam et al., 2019). During transesterification, a significant number of chemical bonds,

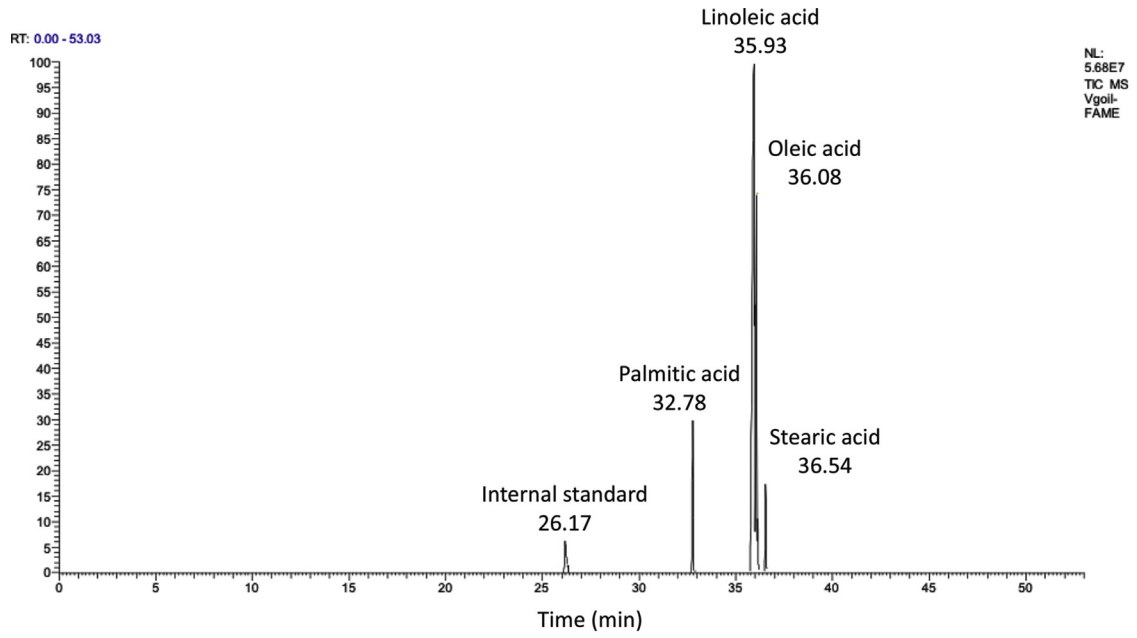

(a)

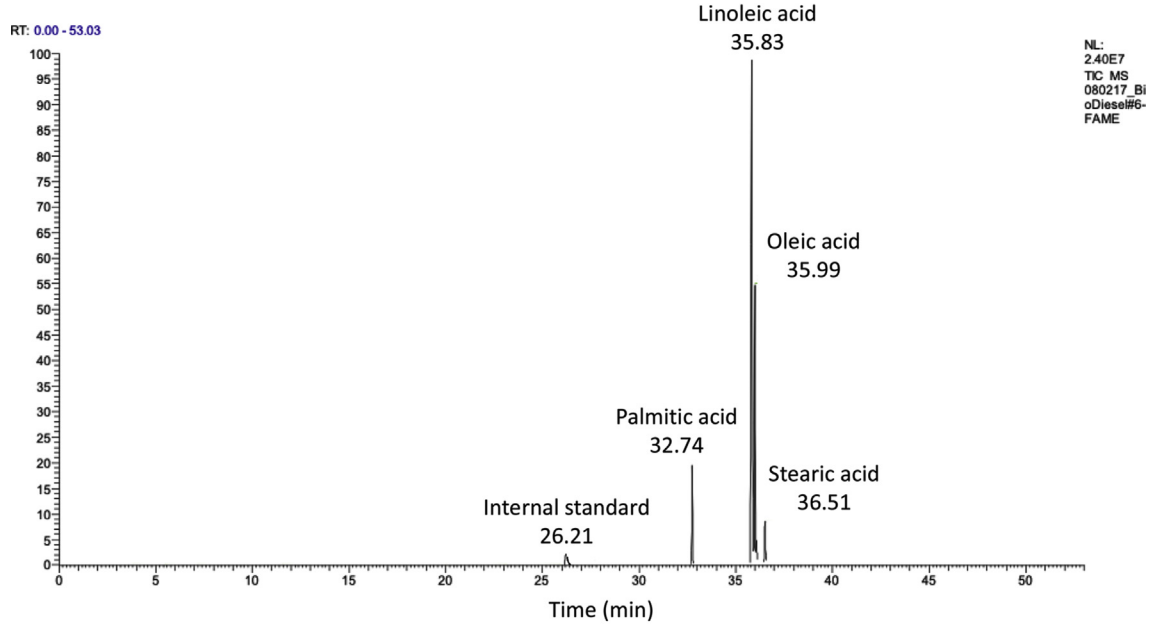

(b)

Fig. 6. The GC spectra of biodieoduced from the conventional transesterification process and the LPPD technology in this study; (a) analysis of biodiesel produced from commercial production line, (b) analysis of biodiesel produced from the LPPD process.

such as those between glycerol and methyl esters (C-O), between glycerides (C-C), and between carbon and hydrogen (C-H), need to be broken apart and new bonds need to be formed. The rates of forming the new bonds are governed by the rates of establishing equilibriums between the reactants and products, which is in fact the stage where most of the reaction time is allocated to obtain higher conversion efficiencies (Vasudevan and Briggs, 2008). Therefore, based on the above discussion, it might be hypothesized that the novel LPPD process examined in this study also employed the mechanism of conventional transesterification to produce biodiesel. What was different here was that the LPPD was able to significantly accelerate all the reactions involved in

Table 5
Characteristics of biodiesel produced by the LPPD process (per MEG Corp Consulting).

Parameter	Result of the biodiesel sample in this study	Specification (ASTM D6751)
[a]API Gravity	28.4	Report (D288)
Cloud Point	−1.67 °C	Report (D2500, -3.3 − 15 °C)
Water (Karl Fisher method)	670 ppm	Report (D2709)
Oxidation Stability	>12 h	>3 h (EN14112)
Total Acid Number	0.42 mg KOH g^{-1}	<0.50 mg KOH/g (D664)
Free Glycerin	0.001%	<0.20% mass max (D6584)
Total Glycerin	0.082%	<0.24% mass max (D6584)

[a] API: American Petroleum Institute.

transesterification to reach equilibriums, thus substantially increasing the overall reaction rate of this process. Nonetheless, this hypothesis cannot be verified with the data obtained from this study. Further research is thus needed to closely examine the various reaction processes happening during the electrical plasma discharge period to understand the mechanism in accelerating the transesterification rate.

In addition, the quality of the biodiesel produced using the LPPD technology could be considered meeting the current industrial standards of the biodiesel industry. Based on the analysis results, there was virtually no difference existing between biodiesel samples obtained from the commercial production line and the LPPD in this study (Fig. 6). This conclusion could also be obtained based on comparing the results of a biodiesel sample produced by the LPPD process (Table 5) with the ASTM standards (Knothe, 2006).

Finally, the limited data obtained from this study were insufficient to conduct a full-fledged economic analysis on the LPPD process in producing biodiesel from soybean oil as compared to the conventional technique. However, a brief estimate of the electricity consumption might be calculated to shed some light on the advantages of the new system. For producing 1 L of biodiesel, the electrical energy needed to heat the oil to 70 °C for 1 L soybean oil could be calculated as 1.79 kJ/L·K x 50 K = 89.55 kJ, which was equivalent to 0.025 kWh. This was based on the assumption that the specific heat of soybean oil was 1.79 kJ/L·K (Fasina and Colley, 2008) and the room temperature was 20 °C, For the LPPD process, at 2.7 ml s^{-1}, the electrical discharging time was clocked as 0.5 ms (0.0005 s) and the discharging power was recorded to be 0.3 kW. This translated to a power consumption of 0.42 x 10^{-4} kWh for 100 ml soybean oil (or 4.2 x 10^{-4} kWh for 1 L). The power consumption was only 1/600 of the power needed for the conventional technique to increase the temperature of 1 L soybean oil to the reaction temperature range (60–80 °C). Please note that this is only for raising the temperature, not including the additional power usage for the transesterification process. If the latter is factored in, the total power consumption can be much higher. Although simple and rough, this estimate clearly shows the advantage of the novel LPPD system in converting soybean oil into biodiesel from the perspective of electricity savings.

3.4. Challenges in the current research and future work

Summarizing the work presented in this paper can provide an insight on planning and directing future research efforts to meet the challenges ahead. In general, the challenges could come from four areas, i.e., the reactor design (including optimization), reaction mechanism, source of feedstock, and scale-up applications. For reactor design, there are still many unknowns in terms of material selections and reactor configuration. For instance, quartz was selected for the dielectric plate in this study. During the fabrication of the LPPD reactor, it was found that quartz was brittle and easy to crack. Thus, materials with better mechanical, but similar electrical, properties should be sought for manufacturing the dielectric plate. Speaking of reactor configuration, the dimensions of the reactor components, such as the thickness of the dielectric plate (3.2 mm used in this study), the diameter of the discharging pin-hole in the middle of the dielectric plate (0.8 mm used in this study), and the diameter of the reactor can be areas for further research because these parameters are in general considered to have significant impacts on the performance of electrical discharge reactors (Bruggeman et al., 2016). Besides the design of reactor, operating parameters also need to be further evaluated. As stated early, it was found that increasing the flowrate of the LPPD system would not impair the soybean oil conversion rate if the applied voltage was kept under 1.38 kV. Along this line, researching how high the flowrate can go beyond 4.1 ml s^{-1} without negatively impacting the conversion rate will certainly make sense from the perspective of improving the overall system efficiency. For reaction mechanisms, although transesterification was hypothesized as the reaction happening during the plasma discharge period, detailed physical, chemical, and electrical processes involved in accelerating the transesterification rates remain unclear. For the feedstock, it is widely recognized that the feedstock cost constitutes the main obstacle for commercial production of biodiesel from edible vegetable oils (Alalwan et al., 2019). Since only the virgin soybean oil was tested in this study, the capability of the LPPD system to handle other oily feedstocks such as the used cooking oil has yet to be examined. Finally, the most challenging area may belong to the scale-up and commercialization step. Since the LPPD system was designed, with all the experiments conducted, at the lab-scale, future research should focus on developing detailed technical procedures to scale up the system for practical applications. In addition, economic evaluation of the entire system should also be performed and compared to that of the conventional biodiesel production systems.

4. Conclusion

A novel liquid-phase plasma discharge (LPPD) process was evaluated in biodiesel synthesis using soybean oil as substrate. The results included:

- the LPPD process was able to continuously produce biodiesel from soybean oil, thus advancing the currently widely used, batch-based production processes;
- the optimum running conditions for synthesizing biodiesel using the LPPD reactor were 5.08 (methanol to oil molar ratio) and 0.79 (NaOH to oil weight ratio) for flowrate 2.7 ml s^{-1}, and 5.18 and 0.70 for 4.1 ml s^{-1}, based on the analysis using the central composite design and response surface methodology;
- the optimal conversion rates and applied voltages were 97.42% and 1.26 kV for flowrate 2.7 ml s^{-1}, and 99.45% and 1.37 kV for 4.1 ml s^{-1};

- this novel LPPD process can significantly reduce the time and heating energy required for the conventional transesterification reaction, thus having the potential to greatly improve the production efficiency of the current biodiesel industry;
- the technology was only evaluated against the virgin oil, so the results obtained might not be applicable to other oil feedstocks;
- further research is needed to examine its performance in converting other oily substrates into biodiesel to reduce the major production cost, i.e., the feedstock cost, and to scale up.

Acknowledgement

This work is supported by the USDA National Institute of Food and Agriculture, Hatch project IDA01573 and Minnesota Soybean Research and Promotion Council, project 103-6900534.

References

Afzal, A., Kareemullah, M., RK, A.R., 2018. Production of biodiesel from various sources and comparative engine perfor-mance studies by using different biodiesel blends. J. Eng. Res. 6 (4), 1–21.
Akhtatr, T., Tariq, M., Sultana, N., Ahmad, M., 2018. Production of biodiesel by ultrasonic-assisted methanolysis of cantaloupe seed oil and its optimization by taguchi method production. J. Chem. Soc. Pak. 40 (3), 427–436.
Alalwan, H.A., Alminshid, A.H., Aljaafari, H.A., 2019. Promising evolution of biofuel generations. Subject review. Renew. Energy Focus 28, 127–139. https://doi.org/10.1016/j.ref.2018.12.006.
Antolın, G., Tinaut, F.V., Briceño, Y., Castaño, V., Pérez, C., Ramırez, A.I., 2002. Optimisation of biodiesel production by sunflower oil transesterification. Bioresour. Technol. 83 (2), 111–114. https://doi.org/10.1016/S0960-8524(01)00200-0.
Aransiola, E., Ojumu, T., Oyekola, O., Madzimbamuto, T., Ikhu-Omoregbe, D., 2014. A review of current technology for biodiesel production: state of the art. Biomass Bioenergy 61, 276–297. https://doi.org/10.1016/j.biombioe.2013.11.014.
Arumugam, A., Gopinath, K., Anuse, P., Shwetha, B., Ponnusami, V., 2019. Kinetic modelling and techno-economic analysis of biodiesel production from Calophyllum inophyllum oil. Biomass Convers. Biorefinery 1–16 doi.org/10.1007/s1339.
ASTM, 2018. Standard Specification for Biodiesel Fuel Blend Stock (B100) for Middle Distillate Fuels, Designation: D6751 - 18. American Society for Testing and Materials International, West Conshohocken, Pennsylvania, USA.
Attaphong, C., Singh, V., Balakrishnan, A., Do, L.D., Arpornpong, N., Parthasarathy, R.N., Gollahalli, S.R., Khaodhiar, S., Sabatini, D.A., 2016. Phase behaviors, fuel properties, and combustion characteristics of alcohol-vegetable oil-diesel microemulsion fuels. Int. J. Green Energy 13 (9), 930–943.
Azcan, N., Yilmaz, O., 2012. Microwave irradiation application in biodiesel production from promising biodiesel feedstock: microalgae (Chlorella protothecoides). In: Proc. World Congr. Eng. Comput. Sci. San Fransisco, USA.
Babajide, O., Petrik, L., Amigun, B., Ameer, F., 2010. Low-cost feedstock conversion to biodiesel via ultrasound technology. Energies 3 (10), 1691–1703. https://doi.org/10.3390/en3101691.
Bhuiya, M., Rasul, M., Khan, M., Ashwath, N., Azad, A., 2016. Prospects of 2nd generation biodiesel as a sustainable fuel—part: 1 selection of feedstocks, oil extraction techniques and conversion technologies. Renew. Sustain. Energy Rev. 55, 1109–1128. https://doi.org/10.1016/j.rser.2015.04.163.
Borges, M., Díaz, L., 2012. Recent developments on heterogeneous catalysts for biodiesel production by oil esterification and transesterification reactions: a review. Renew. Sustain. Energy Rev. 16 (5), 2839–2849. https://doi.org/10.1016/j.rser.2012.01.071.
Bruggeman, P., Graham, L., Degroote, J., Vierendeels, J., Leys, C., 2007. Water surface deformation in strong electrical fields and its influence on electrical breakdown in a metal pin–water electrode system. J. Phys. D Appl. Phys. 40 (16), 4779.
Bruggeman, P.J., Kushner, M.J., Locke, B.R., Gardeniers, J.G.E., Graham, W.G., Graves, D.B., Hofman-Caris, R., Maric, D., Reid, J.P., Ceriani, E., Fernandez Rivas, D., Foster, J.E., Garrick, S.C., Gorbanev, Y., Hamaguchi, S., Iza, F., Jablonowski, H., Klimova, E., Kolb, J., Krcma, F., Lukes, P., MacHala, Z., Marinov, I., Mariotti, D., Mededovic Thagard, S., Minakata, D., Neyts, E.C., Pawlat, J., Petrovic, Z.L., Pflieger, R., Reuter, S., Schram, D.C., Schröter, S., Shiraiwa, M., Tarabová, B., Tsai, P.A., Verlet, J.R.R., Von Woedtke, T., Wilson, K.R., Yasui, K., Zvereva, G., 2016. Plasma-liquid interactions: a review and roadmap. Plasma Sources Sci. Technol. 25 (5), 053002. https://doi.org/10.1088/0963-0252/25/5/053002.
Canabarro, N., Soares, J.F., Anchieta, C.G., Kelling, C.S., Mazutti, M.A., 2013. Thermochemical processes for biofuels production from biomass. Sustain. Chem. Process. 1 (1), 22. https://doi.org/10.1186/2043-7129-1-22.
Christian, K., Agbangnan, D.C.P., Dominique S, C.K., 2018. Comparative study of transesterification processes for biodiesel production (A review). Appl. Chem. 120, 51235–51242.
Cubas, A.L.V., Machado, M.M., Pinto, C.R.S.C., Moecke, E.H.S., Dutra, A.R.A., 2016. Biodiesel production using fatty acids from food industry waste using corona discharge plasma technology. Waste Manag. 47, 149–154. https://doi.org/10.1016/j.wasman.2015.05.040.
De, R., Bhartiya, S., Shastri, Y., 2019. Multi-objective optimization of integrated biodiesel production and separation system. Fuel 243, 519–532. https://doi.org/10.1016/j.fuel.2019.01.132.
Di Serio, M., Tesser, R., Pengmei, L., Santacesaria, E., 2007. Heterogeneous catalysts for biodiesel production. Energy Fuel. 22 (1), 207–217. https://doi.org/10.1021/ef700250g.
Draper, N.R., Smith, H., 1998. Applied Regression Analysis, third ed. ed. Wiley-Interscience, New York.
Eevera, T., Rajendran, K., Saradha, S., 2009. Biodiesel production process optimization and characterization to assess the suitability of the product for varied environmental conditions. Renew. Energy 34 (3), 762–765. https://doi.org/10.1016/j.renene.2008.04.006.
EN, 2016. Fat and Oil Derivatives - Fatty Acid Methyl Esters (FAME) - Determination of Oxidation Stability (Accelerated Oxidation Test). The European Committee for Standardization, Brussels, Belgium.
Fasina, O., Colley, Z., 2008. Viscosity and specific heat of vegetable oils as a function of temperature: 35 C to 180 C. Int. J. Food Prop. 11 (4), 738–746. https://doi.org/10.1080/10942910701586273.
Indarti, E., Majid, M.I.A., Hashim, R., Chong, A., 2005. Direct FAME synthesis for rapid total lipid analysis from fish oil and cod liver oil. J. Food Compos. Anal. 18 (2–3), 161–170. https://doi.org/10.1016/j.jfca.2003.12.007.
Istadi, I., Yudhistira, A.D., Anggoro, D.D., Buchori, L., 2014. Electro-catalysis system for biodiesel synthesis from palm oil over dielectric-barrier discharge plasma reactor. Bull. Chem. React. Eng. Catal. 9 (2), 111. https://doi.org/10.1016/j.jfca.2003.12.007.
Jeyakumar, N., Narayanasamy, B., Balasubramaniam, V., 2018. Optimization of used cooking oil methyl ester production using response surface methodology. Energy Sources, Part A Recovery, Util. Environ. Eff. 1–13. https://doi.org/10.1080/15567036.2018.1555633.
Jiang, B., Zheng, J., Qiu, S., Wu, M., Zhang, Q., Yan, Z., Xue, Q., 2014. Review on electrical discharge plasma technology for wastewater remediation. Chem. Eng. J. 236, 348–368. https://doi.org/10.1016/j.cej.2013.09.090.
Joshi, S., Hadiya, P., Shah, M., Sircar, A., 2019. Techno-economical and experimental analysis of biodiesel production from used cooking oil. Biophys. Econ. Res. Qual. 4 (1), 2. https://doi.org/10.1007/s41247-018-0050-7.
Knothe, G., 2006. Analyzing biodiesel: standards and other methods. J. Am. Oil Chem. Soc. 83 (10), 823–833. https://doi.org/10.1007/s11746-006-5033-y.
Laesecke, J., Ellis, N., Kirchen, P., 2017. Production, analysis and combustion characterization of biomass fast pyrolysis oil–Biodiesel blends for use in diesel engines. Fuel 199, 346–357. https://doi.org/10.1016/j.fuel.2017.01.093.
Lehmann, E.L., Romano, J.P., 2008. Testing Statistical Hypotheses. Springer, New York.
Lesage, O., Falk, L., Tatoulian, M., Mantovani, D., Ognier, S., 2013. Treatment of 4-chlorobenzoic acid by plasma-based advanced oxidation processes. Chem. Eng. Process: Process Intensification 72, 82–89. https://doi.org/10.1016/j.cep.2013.06.008.
Li, Y., Ye, B., Shen, J., Tian, Z., Wang, L., Zhu, L., Ma, T., Yang, D., Qiu, F., 2013. Optimization of biodiesel production process from soybean oil using the sodium potassium tartrate doped zirconia catalyst under Microwave Chemical Reactor. Bioresour. Technol. 137, 220–225. https://doi.org/10.1016/j.biortech.2013.03.126.
Mendenhall, W., Sincich, T., 2012. A Second Course in Statistics: Regression Analysis, seventh ed. Prentice Hall, Upper Saddle River, NJ, USA.
Moazeni, F., Chen, Y.-C., Zhang, G., 2019. Enzymatic transesterification for biodiesel production from used cooking oil, a review. J. Clean. Prod. 216, 117–128. https://doi.org/10.1016/j.jclepro.2019.01.181.
Mohammed, A.R., Bhargavi, R., 2015. Biodiesel production from waste cooking oil. J. Chem. Pharm. Res. 7 (12), 670–681.
Musa, I.A., 2016. The effects of alcohol to oil molar ratios and the type of alcohol on biodiesel production using transesterification process. Egypt. J. Petrol. 25 (1), 21–31. https://doi.org/10.1016/j.ejpe.2015.06.007.
Nasreen, S., Nafees, M., Qureshi, L.A., Asad, M.S., Sadiq, A., Ali, S.D., 2018. Review of Catalytic Transesterification Methods for Biodiesel Production. Biofuels-State of Development. IntechOpen, pp. 93–119. https://doi.org/10.5772/intechopen.75534.
Noureddini, H., Zhu, D.Y., 1997. Transesterification of soybean oil. J. Am. Oil Chem. Soc. 74, 1457–1463.
Oğuz, H., Tolu, M.Ç., 2018. A review on biodiesel production using eggshell as catalyst. Int. J. Eng. Adv. Technol. 5 (3), 147–152. https://doi.org/10.31593/ijeat.445819.
Osman, N.B., McDonald, A.G., Laborie, M.-P.G., 2012. Analysis of DCM Extractable Components from Hot-Pressed Hybrid Poplar. https://doi.org/10.1515/hf-2012-0011.
Patinglag, L., Sawtell, D., Iles, A., Melling, L., Whitehead, K., Shaw, K., 2018. Evaluation of a microfluidic atmospheric-pressure plasma reactor for water treatment. In: International Symposium on Non-Thermal/Thermal Plasma Pollution Control Technology and Sustainable Energy (ISNTP-11). Manchester Metropolitan University, Padova, Italy.
Santos, F.F.P., Rodrigues, S., Fernandes, F.A.N., 2009. Optimization of the production of biodiesel from soybean oil by ultrasound assisted methanolysis. Fuel Process. Technol. 90 (2), 312–316. https://doi.org/10.1016/j.fuproc.2008.09.010.
Silva, G.F., Camargo, F.L., Ferreira, A.L.O., 2011. Application of response surface

methodology for optimization of biodiesel production by transesterification of soybean oil with ethanol. Fuel Process. Technol. 92 (3), 407–413. https://doi.org/10.1016/j.fuproc.2010.10.002.

Sugai, T., Nguyen, P.T., Tokuchi, A., Jiang, W., Minamitani, Y., 2015. The effect of flow rate and size of water droplets on the water treatment by pulsed discharge in air. IEEE Trans. Plasma Sci. 43 (10), 3493–3499. https://doi.org/10.1109/TPS.2015.2450741.

Tan, S.X., Lim, S., Ong, H.C., Pang, Y.L., 2019. State of the art review on development of ultrasound-assisted catalytic transesterification process for biodiesel production. Fuel 235, 886–907. https://doi.org/10.1016/j.fuel.2018.08.021.

Thanh, L.T., Okitsu, K., Boi, L.V., Maeda, Y., 2012. Catalytic technologies for biodiesel fuel production and utilization of glycerol: a review. Catalysts 2 (1), 191–222. https://doi.org/10.3390/catal2010191.

Thoai, D.N., Tongurai, C., Prasertsit, K., Kumar, A., 2019. Review on biodiesel production by two-step catalytic conversion. Biocatalysis Agric. Biotechnol. 101023. https://doi.org/10.1016/j.bcab.2019.101023.

Vasudevan, P.T., Briggs, M., 2008. Biodiesel production—current state of the art and challenges. J. Ind. Microbiol. Biotechnol. 35 (5), 421. https://doi.org/10.1007/s10295-008-0312-2.

Wu, S., Yang, H., Hu, J., Shen, D., Zhang, H., Xiao, R., 2017. The miscibility of hydrogenated bio-oil with diesel and its applicability test in diesel engine: a surrogate (ethylene glycol) study. Fuel Process. Technol. 161, 162–168. https://doi.org/10.1016/j.fuproc.2017.03.022.

Yin, J.-Z., Xiao, M., Song, J.-B., 2008. Biodiesel from soybean oil in supercritical methanol with co-solvent. Energy Convers. Manag. 49 (5), 908–912. https://doi.org/10.1016/j.enconman.2007.10.018.